Dynamic Analysis of a Box Girder Bridge

Analyse dynamique d'un pont à poutres en caisson

Dynamische Berechnung einer Kastenträgerbrücke

MARVIN JONES, Ph.D.
Project Engineer, FMC Corp.
Environment Equipment Division
Chicago, Illinois U.S.A.

KUANG HAN CHU, Ph.D.
Professor of Civil Engineering
Illinois Institute of Technology
Chicago, Illinois U.S.A.

The main purpose of this paper is to present numerical results obtained from a computer program based on a theoretical formulation for the analysis of dynamic effects due to moving loads on deflections, stresses and moments in all plate elements in a simply supported box girder bridge presented in a previous paper [7]. It mainly consists of two parts: (a) verification of the computer program and (b) analysis of an example bridge.

Verification of the computer program was necessary not only to check out the program but to find out the minimum number of plate strips, the minimum number of modes and the largest time increment to be taken for obtaining reasonable accurate results. It was done by comparing the results of the proposed method with those obtained by existing methods or with examples taken from published articles. For a check of natural frequencies and the static solution obtained, simply supported rectangular plates with various aspect ratios and subjected to a load at the center were examined. For a check of the dynamic solution, a slab bridge subjected to a moving load without spring and a beam bridge subjected to a wheel load consisting of both sprung and unsprung masses were checked with existing solutions. Results of static solution of a box girder bridge were compared with those obtained with existing methods. Since the proposed method is based on mode superposition, frequencies and mode shapes of various mode were obtained for the example bridge.

Dynamic analysis were performed for the same box girder bridge considered in the verification for the static solution. Five loading cases were investigated. The first four loading cases are: (a) single load moving along the bridge centerline, (b) single load moving along the curb, (c) two-axle truck moving along the bridge centerline and (d) two-axle truck moving along the curb. All wheel loads are spring borne, of the same magnitude and without initial deflection. The fifth loading case (e) is the same as loading case (c) except that the spring has an initial deflection. Typical history curves showing amplification factors for deflections, longitudinal stresses and plate moments are shown. Impact factors at various points for various loading cases are given in tables.

The amplification factors Λ_d and Λ_s for each dynamic response (deflection, stress or moment, etc.) Γ_d and each static response Γ_s at a specific point are defined respectively as

$$\Lambda_d = \frac{\Gamma_d}{\Gamma_{sm}}, \quad \Lambda_s = \frac{\Gamma_s}{\Gamma_{sm}} \qquad (1a, b)$$

in which Γ_{sm} is the maximum static response at the point. The impact factor I is defined as

$$I = \max |\Lambda_d| - 1 \qquad (2)$$

The motivation of making this study and relevant references were given in the previous paper [7]. The following items are also pointed out in that paper but they are repeated herein as they involve basic assumptions or definitions of relevant symbols.

1. The truck is simplified into one with two identical axle loads 14 ft. (4.26 m) apart [1]. Each axle consists of two identical wheel loads which are at 6 ft. (1.83 m) apart [1] and represented by spring supported masses with the force in the spring distributed over a rectangular area (see Fig. 1). Unsprung masses and internal damping of the wheel loads are neglected as their effects are relatively small (4, 8, 9).

2. The box girder bridge is simply supported with span length L and consists of a number of plate elements. As shown in Fig. 2, each plate element is further divided into several plate strips and consistant masses [3] are applied along the line joining the strips. The x axis is taken along the longitudinal direction of the bridge and has its origin at the left end of the bridge. The y direction is taken as perpendicular to x in the plane of any plate strip. Positive directions of longitudinal stress σ_x and plate moments M_x and M_y (moment per unit width) in a plate element of thickness $\bar{t}$ are shown in Figure 3. Symbols for other force and moment resultants shown in Figure 3 are not given as they are not involved in this paper.
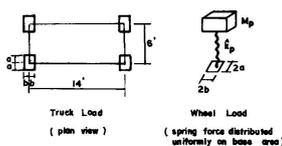
Fig. 1. Simplified Live Load.
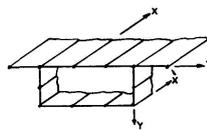
Fig. 2. Plate Element in a Box Girder Bridge.
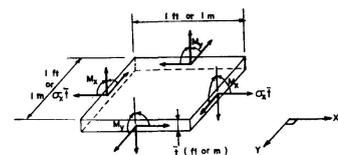
Fig. 3. Positive Directions for σ_x, M_x and M_y (Symbols are Omitted for Stress Resultants not Involved Herein).

3. The bridge is considered as having negligible structural damping [14] and it is supposed to satisfy the following main assumptions of folded plate analysis. (a) Plate elements are perfectly elastic, rectangular in shape and rigidly jointed along longitudinal edges. (b) The transverse end of the plates are framed into diaphragms which are flexible normal to their own plane but infinitely stiff in their own plane. (c) No interaction exists between bending resisting forces (moments and transverse shears) and membrane forces.

Verification of the Computer Program

As stated in the introduction, the purpose of verifying the computer program is not only to check out the program but to find out the minimum number of plate strips, the minimum number of modes and the largest time increment to be taken for obtaining reasonable accurate results. Numerical results obtained for the various case considered are presented in the following.

Natural Frequencies and Static Solution of Centrally Loaded Rectangular Plates

Natural frequencies and static solutions for centrally loaded simply supported rectangular plates were obtained. The concentrated load investigated is 25 k (111.2 kN) distributed on an area of 4.5' × 4.5' (1.38 m × 1.38 m). The plate thickness (t) is 8" (20.32 cm); the modulus of elasticity (E) is 432×10^3 ksf (3×10^6 psi or 206×10^3 kN/cm²) and the Poisson's ratio (μ) is 0.3. The dimensions of the plates, numbers of plate elements used, the first 3 transverse mode frequencies, numbers of modes taken, moments and deflections under the load are given in Table 1, which shows the comparison of results of the proposed method with those of the series solution given by TIMOSHENKO's books [15, 16].

Table 1. Comparison of Results of the Proposed Method (a) with those of the Series Solution (b) for Centrally Loaded Simply Supported Rectangular Plates

Plate Size (ft.)	$\frac{L}{B}$	No. of Elem.	\multicolumn{6}{c}{Natural Frequencies}	No. of Modes Included		\multicolumn{6}{c}{Values at the Center of the Plate}
			\multicolumn{2}{c}{$\frac{1}{\omega^2} \times 10^3$}	\multicolumn{2}{c}{$\frac{1}{\omega^2} \times 10^4$}	\multicolumn{2}{c}{$\frac{1}{\omega^2} \times 10^5$}			\multicolumn{2}{c}{M_x (k ft/ft)}	\multicolumn{2}{c}{M_y (k ft/ft)}	\multicolumn{2}{c}{Defl. (ft)}
			(a)	(b)	(a)	(b)	(a)	(b)	n	m	(a)	(b)	(a)	(b)	(a)	(b)
31.5 x 22.5	1.5	5	.3279	.3281	.3663	.3678	.8129	.8273	9	7	3.789	5.218	5.292	6.014	.0145	.0152
45.0 x 22.5	2.0	5	.4787	.4788	.4127	.4142	.8100	.8745	9	7	3.746	5.075	5.711	6.300	.0163	.0169
45.0 x 22.5	2.0	8	.4788	.4788	.4140	.4142	.8721	.8745	9	7	4.069	5.075	6.048	6.300	.0163	.0169
45.0 x 22.5	2.0	8	.4788	.4788	.4140	.4142	.8721	.8745	15	8	3.942	5.075	5.953	6.300	.0163	.0169
75.0 x 22.5	3.3	5	.6296	.6298	.4457	.4473	.8910	.9055	9	7	3.464	5.053	5.544	6.429	.0168	.0174
90.0 x 22.5	4.0	5	.6626	.6628	.4518	.4534	.8965	.9110	9	7	3.268	5.052	5.383	6.431	.0167	.0174
90.0 x 22.5	4.0	8	.6627	.6628	.4531	.4534	.9086	.9110	9	7	3.640	5.052	5.919	6.431	.0167	.0174
90.0 x 22.5	4.0	8	.6627	.6628	.4531	.4534	.9086	.9110	15	8	3.968	5.052	6.090	6.431	.0168	.0174
135.0 x 22.5	6.0	5	.7081	.7083	.4597	.4612	.9035	.9180	9	7	2.644	5.052	4.790	6.431	.0161	.0174
281.2 x 22.5	12.5	5	.7386	.7387	.4646	.4661	.9079	.9224	9	7	1.413	5.052	3.384	6.431	.0128	.0174
281.2 x 22.5	12.5	8	.7387	.7387	.4659	.4661	.9200	.9224	9	7	1..509	5.052	3.623	6.431	.0128	.0174
281.2 x 22.5	12.5	8	.7387	.7387	.4659	.4661	.9200	.9224	15	8	2.358	5.052	4.725	6.431	.0152	.0174

1 ft = 0.3048 m   1 k-ft/ft = 4.448 kN-m/m

From Table 1, it can be seen that in general the accuracy of the frequencies are fairly good. For the number of modes considered, the deflections are also checked very well with the series solution except for long plates with $L/B \geq 6$. The M_x and M_y values at points away from the concentrated load generally show fairly good agreement as will be shown in another example. However, the M_x and M_y values at center of application of the load depend on the length to width ratio (L/B) of the plate, number of plate elements (n_s) and number of modes (m and n) taken into consideration.

At the point under the concentrated load, for a plate with $L/B = 2$, $n_s = 5$, $n = 9$ and $m = 7$, the M_y value is 90% of the series solution but M_x value is only 74% of the series solution. For the same plate with $n_s = 8$, $n = 9$, and $m = 7$, the M_y value is 96% and the M_x value is 80% of the series solution. Thus improved accuracy is obtained with more plate elements. However, for the same plate with $n_s = 8$, $n = 15$ and $m = 8$, the M_x and M_y values are slightly worse than the case of $n_s = 8$, $n = 9$ and $m = 7$. This loss of accuracy with the inclusion of higher modes is undoubtedly due to the inaccuracies in the eigenvectors of the higher modes. The case of $L/b = 4$ is similar to the case of $L/B = 2$ except that M_x and M_y values show improvement as higher modes are included. Unfortunately, for a given number of n_s, n and m, as L/B increases, the accuracy of the M_x and M_y deteriorates. For a plate with $L/B = 12.5$, $n_s = 8$, $n = 9$ and $m = 7$ the value of M_y is 56% of the series solution and that of M_x is only 30% of the series solution. For the same plate with $n_s = 8$, $n = 15$ and $m = 8$, M_y becomes 73% of the series solution and M_x is 46.5% of the series solution.

It becomes evident that reliable moments at point of application of the concentrated load cannot be obtained for long narrow plates unless (a) large number of plate elements are used, (b) large number of higher modes are included, and (c) accurate frequencies and mode shapes can be obtained for higher modes. This becomes impractical particularly under dynamic conditions in that the time increment for numerical integration becomes so short (for convergence, the time increment must be about 1/10 of the period of the highest mode included) that the required computer time for a single loading case becomes unwieldy.

Verification of the Dynamic Solution of a Slab Bridge and a Beam Bridge

A check of the dynamic solution is made for a slab bridge subjected to an unsprung moving load analyzed by IYENGAR and JAGADISH [11] and a beam bridge subjected to a sprung load attached to an unsprung load by EICHMANN [9]. Excellent agreements were obtained except for the moment M_x at center of slab bridge in that the original paper was believed in error.

Static Solution and Vibration Modes of a Box Girder Bridge

The static solution of a box girder bridge under a concentrated load is compared with that obtained by the well known elasticity method (6, 10, 13). Figure 4 shows the cross-section of the example bridge which is simply supported with 100 ft. (30.48 m) span. The mass density (ρ) is taken as .005 k-sec^2/ft^4; (161 pcf weight or 2570 kg/m^3) the modulus of elasticity (E) as 432×10^3 ksf (3×10^6 psi or 206×10^3 kN/cm^2) and Poisson's ratio (μ) as 0.2.

The concentrated load is 25 k (111 kN) applied on an area of $24'' \times 8''$ (61 cm $\times$ 20.3 cm) with $24''$ in the transverse and $8''$ in the longitudinal direction of the bridge. Two load cases are considered: (a) load applied at midspan of the centerline of the bridge (b) load applied at midspan with edge of the load touching inside of the right curb (see Fig. 9).

Plate elements used for analysis of the example bridge are as shown in Figure 5. The curb section is considered as a thick plate element which has the same centroidal

axis as the top slab. This will result in apparent discontinuity in the slab bending stress corresponding to M_x at the junction of the curb and the top slab. This discontinuity can be removed if eccentricity of the curb section is taken into consideration.
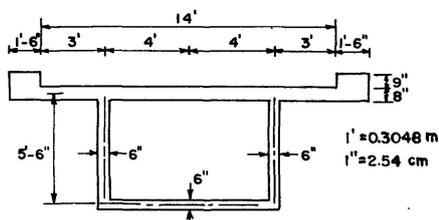
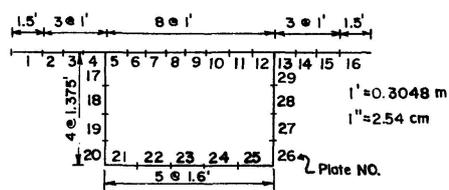

Fig. 4. The Example Bridge.
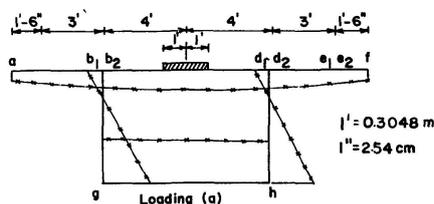

Fig. 5. Plate Elements Used
for the Example Bridge.
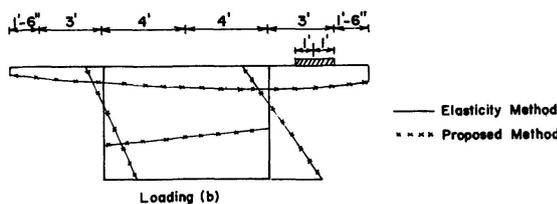
Fig. 6. Static Loading Cases
and Longitudinal Stress Distribution.

The mode shapes of the first eight transverse modes (m = 1 to 8, n = 1) are as shown in Figure 7 and the frequencies and period of all the modes up to m = 8, n = 15 are given in Table 2. The computer running time for obtaining these frequencies and mode shapes is 20.0 min. on Univac 1108. It should be noted that the first mode frequency for the corresponding simply supported beam with cross-sectional area = 23.0 ft^2 (2.14 m^2) and moment of inertia = 124.0 ft^4 (1.07 m^4) is 21.3 as compare with 20.02 as shown in Table 2.

Table 2. *Circular Frequencies and Periods of the Various Modes of the Example Bridge*

		n = 1	n = 2	n = 3	n = 4	n = 5	n = 6	n = 7	n = 8	n = 9	n = 10	n = 11	n = 12	n = 13	n = 14	n = 15
m = 1	ω	20.02	71.84	134.4	188.7	234.1	276.7	319.8	362.7	399.8	429.2	456.9	485.8	517.0	550.6	586.9
	τ	.3138	.0875	.0467	.0333	.0268	.0227	.0196	.0173	.0157	.0146	.0138	.0129	.0122	.0114	.0107
m = 2	ω	80.66	118.3	154.3	197.9	244.3	291.5	340.3	392.0	438.8	488.1	544.4	602.7	659.7	714.4	768.3
	τ x 10	.7790	.5312	.4071	.3174	.2572	.2155	.1846	.1603	.1432	.1287	.1154	.1043	.0952	.0880	.0818
m = 3	ω	151.7	177.1	218.3	272.0	321.4	354.1	469.4	403.1	447.8	508.7	638.8	689.4	738.7	817.5	906.8
	τ x 10	.4142	.3548	.2878	.2310	.1955	.1775	.1338	.1559	.1403	.1235	.0984	.0911	.0851	.0769	.0693
m = 4	ω	266.6	296.1	353.5	367.0	390.7	427.7	471.0	510.4	551.0	592.9	575.1	647.7	830.9	916.8	962.3
	τ x 10	.2357	.2122	.1777	.1712	.1608	.1469	.1335	.1231	.1140	.1060	.1092	.0970	.0756	.0685	.0653
m = 5	ω	342.6	346.4	348.0	423.8	517.5	620.7	726.1	827.8	920.2	999.2	1064	1107	1165	1211	1255
	τ x 10	.1834	.1814	.1806	.1483	.1214	.1012	.0865	.0759	.0683	.0628	.0591	.0568	.0539	.0519	.0501
m = 6	ω	625.4	641.3	673.0	724.1	796.2	887.2	992.5	1107	1175	1226	1287	1358	1421	1492	1560
	τ x 10	.1005	.0980	.0934	.0868	.0789	.0708	.0633	.0567	.0535	.0513	.0488	.0463	.0442	.0421	.0403
m = 7	ω	963.6	1005	1026	1041	1058	1078	1103	1134	1227	1350	1474	1597	1714	1839	1955
	τ x 10^2	.6520	.6251	.6126	.6035	.5940	.5830	.5698	.5539	.5119	.4653	.4262	.3936	.3664	.3416	.3214
m = 8	ω	1216	1254	1295	1341	1391	1455	1509	1575	1648	1728	1816	1920	2027	2124	2391
	τ x 10^2	.5166	.5009	.4851	.4687	.4515	.4334	.4164	.3989	.3813	.3637	.3461	.3272	.3098	.2958	.2628

τ = 2π/ω sec.

A comparison of the results obtained by the elasticity method [6] with those by the proposed method is shown in Table 3 and in Figures 6 and 8. It can be seen that fairly good agreement of deflections, longitudinal stresses and plate moments is obtained at all points except those directly under the load. From the previous results of the centrally loaded simply supported plates, this lack of agreement for the response under the load is not unexpected.
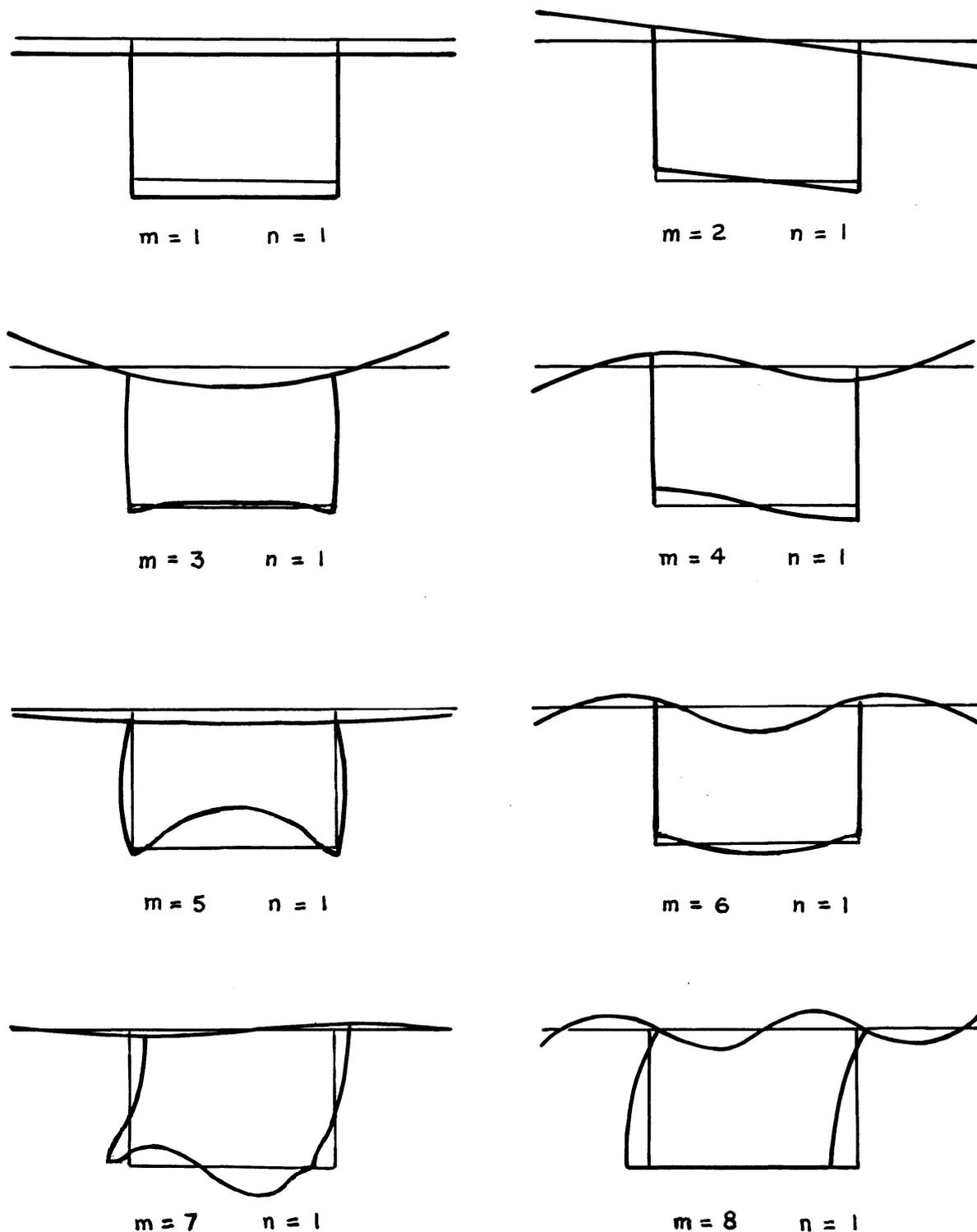

Fig. 7. Mode Shapes for the Example Bridge.

Table 3. Comparison of Results of the Elasticity Method and the Proposed Method for Points on the Cross Section at Midspan of the Bridge

Static Loading Case (a)

Method	Deflection (ft)			Long. Stress (ksf)			M_x (k-ft/ft)				M_y (k-ft/ft)			
	a,f	b,d	g,h	a,f	b,d	g,h	a,f	b_1,d_2	b_2,d_1	c	a,f	b_1,d_2	b_2,d_1	c
Elasticity	.0101	.0109	.0109	-7.46	-8.97	21.09	.20	-.01	-.20	4.95	0	-1.00	-1.94	5.85
Proposed	.0101	.0109	.0109	-7.80	-8.63	21.35	.33	-.02	-.22	1.43	0	-1.09	-1.94	2.78

Static Loading Case (b)

Method	Deflection (ft)						Longitudinal Stress (ksf)					
	a	b	d	f	g	h	a	b	d	f	g	h
Elasticity	.0098	.0101	.0118	.0144	.0100	.0117	-6.95	-7.21	-10.34	-8.24	16.00	25.33
Proposed	.0098	.0101	.0118	.0145	.0100	.0117	-6.88	-7.64	-10.81	-8.19	15.68	25.66

Static Loading Case (b)

Method	M_x (k-ft/ft)						M_y (k-ft/ft)					
	a	b_1 b_2	c	d_1 d_2	e_1 e_2	f	a	b_1 b_2	c	d_1 d_2	e_1 e_2	f
Elasticity	1.13	0.12 / 0.06	-.06	-.05 / -.40	0.95 / 6.91	7.05	0	.09 / -.19	-.56	-1.49 / -3.20	1.33 / 1.33	0
Proposed	1.29	0.13 / 0.06	-.08	-.07 / -.23	0.93 / 6.54	7.33	0	.11 / -.21	-.69	-0.82 / -2.37	1.42 / 1.56	0

1 ft = 0.3048 m,   1 ksf = 0.4788 kN/cm², 1 k-ft/ft = 4.448 kN-m/m

Dynamic Analysis of an Example Bridge

The example bridge considered is the same as shown in Figure 4 with the same span length and material properties as given previously. Five loading cases are considered. The first four cases are as shown in Figure 9: (a) single spring borne load along the bridge centerline, (b) single spring borne load along the inside of the right curb, (c) two axles (4 spring borne loads) 14 ft. (4.26 m) apart with their centerline coinciding with the bridge centerline, (d) two axles (4 spring borne loads) 14 ft. apart with exterior wheel touching the inside of the right curb. The fifth loading case (e) will be introduced later.

Each wheel load is taken as 16 k [71.2 kN see reference [1]] distributed over an area of 24" (61 cm) transverse by 8" (20.3 cm) longitudinal (83.3 psi tire pressure). The data represent a compromise of the data given in references [2] and [12]. The wheel load is considered a spring borne mass with a spring constant of 104 k/ft. (15.2 kN/cm) [see references [8] and [9]]. The speed (V) of the loads is taken as 100 ft/sec. (30.48 m/sec. or 68 miles per hr.). The springs are considered as starting at zero vertical displacement and zero velocity when the load is entering the bridge.

An examination of Table 2 shows that as expected, the frequency becomes higher and the period becomes shorter as m and n increase. In order to obtain convergence for dynamic analysis, it was found by trial that the time increment should be about 1/10 of the shortest period. At m = 8 and n = 15, the period is .0026 which would need excessive time for computer runs. By trial, it was found that

including the modes up to m = 6 and n = 9 would give static moments which agree fairly well with those obtained by the elasticity method at all points except those directly under the load. (The static plate moments for m = 5 may even differ in sign with the corresponding values from the elasticity method). That this being true can also be seen from the mode shapes shown in Figure 7 wherein third mode is included for the top plate only if m = 6. The time increment is .0005 sec. which is 1/10th of the period of the highest mode. The computer running time for a single load case is 192 sec. on Univac 1108. This computer time would be doubled if 4 loads are taken into consideration. Modes up to m = 6 and n = 15 have been included for loading case (a). The computer running time is 696 sec. with time increment of .00035 sec. (Time for evaluating the eigenvalues and vectors are not included in the computer running time).
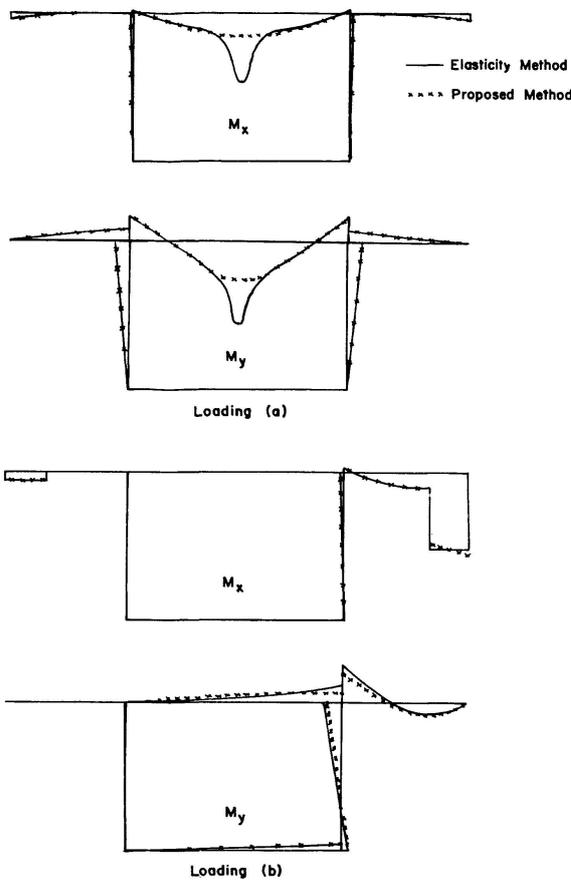

Fig. 8. Distribution of M_x and M_y
by the Elasticity Method
and the Proposed Method.
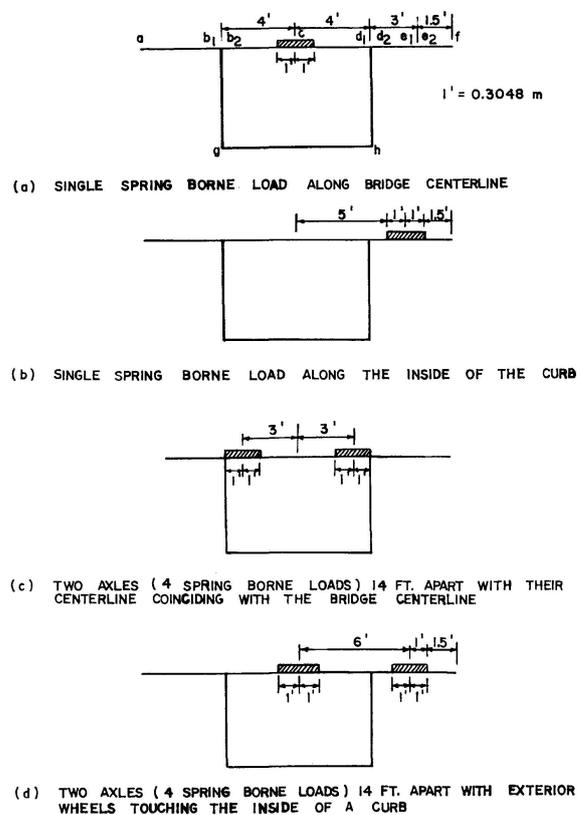
Fig. 9. Dynamic Loading Cases.

For the loading case (a), history curves for the static and dynamic amplification factors are shown in Figure 10 for the midspan deflection and longitudinal stress at point b or d shown in Figure 9a. Amplification factors for the respective midspan M_x and M_y at point b_1 or d_2 are shown in Figure 11. Impact factors at various points on the cross section at midspan shown in Figure 9a are given in Table 4. It can be seen that the maximum impact factor is about 19% for deflection, 16% for longitudinal stress, 4.8% for M_x and 1.3% for M_y.

Fig. 10. History Curves for Midspan Deflection and Longitudinal Stress at Point b or d in fig. 9a, Loading Case (a).

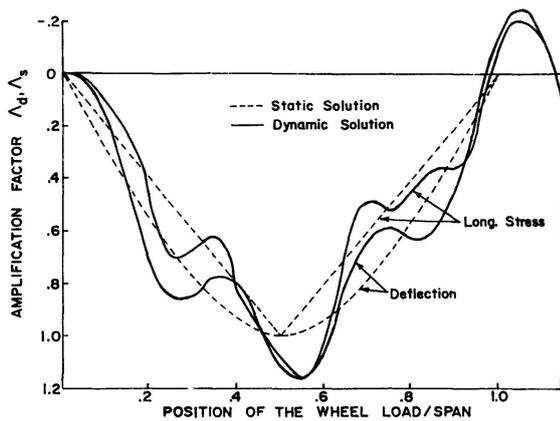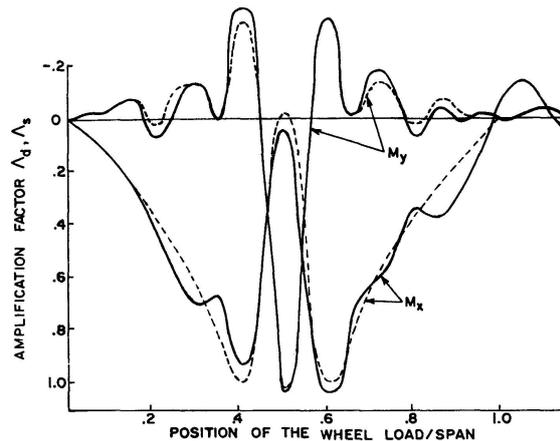Fig. 11. History Curves for Midspan M_x and M_y at Point b_1 or d_2 in Fig. 9a, Loading Case (a).

Impact factors at various points on the midspan section shown in Figure 9a for the loadings (b), (c) and (d) are given in Tables 4 to 6. It can be seen that for loading case (b) the maximum impact factor is about 19% for both deflection and longitudinal stress. The former is the same as for loading case (a) but the latter is higher. Except for M_x at point a the maximum impact factor for both M_x and M_y is slightly less than 4%. The former is somewhat lower than that for case (a) and the latter is somewhat higher. It may be worth noting that M_x at the point which is on the opposite side of the load in an unsymmetrical loading case such as point a in loading cases (b) and (d) always have high impact factor. [19% for loading (b) 6.8% for loading (d)].

Table 4. Impact Factor in Percentages for Loading Cases (a) and (c)

Loading & Modes	(a) m = 6, n = 15				(c) m = 6, n = 9			
Point Fig. 9a	a,f	b_1, d_2 b_2, d_1	c	g,h	a,f	b_1, d_2 b_2, d_1	c	g,h
Defl.	18.81	15.81	9.77	16.65	4.73	4.60	4.57	4.60
Long. Stress	10.84	15.80	8.46	15.43	4.43	4.36	4.43	4.31
M_x	-4.24**	4.80 -3.87	1.84	*	4.20	3.63 3.52	1.83	1.77
M_y	0	1.30 1.32	1.14	*	0	22.18 7.66	2.51	*

*Static value too small to give meaningful results.
**Negative sign indicates that the maximum dynamic moment is smaller than the maximum static moment.

Table 5. Impact Factor in Percentages for Loading Case (b) (mode included m = 6, n = 9)

Point Fig. 9a	a	b_1 b_2	c	d_1 d_2	e_1 e_2	f	g	h
Defl.	19.30	17.91	17.00	15.31	13.25	12.59	17.89	15.05
Long. Stress	10.05	9.68	8.90	12.13	13.35	13.18	18.60	12.07
M_x	19.16	*	-5.88	* -1.99	2.51 2.73	2.58	*	3.93
M_y	0	* 1.70	2.56	3.76 1.03	1.85 1.78	0	.34	.48

*Static value too small to give meaningful results.

With few exceptions [M_y at b for loading (c) and M_x at a for loading (d)], the maximum impact factor for both M_x and M_y for loading cases (c) and (d) with 4-wheel loads is about 4 to 5% which is of the same order of magnitude as that for the single load cases (a) and (b). On the other hand, the maximum impact for both deflection and longitudinal stress for loading cases (c) and (d) is about 4.5 to 5% which is only ¼ to ⅓ of that for loading cases (a) and (b).

It might be of interest to compare the impact factor obtained with that given by the AASHO Specification [1] $I = \dfrac{50}{L + 125} = 22.2\%$ for L = 100 ft. (30.48 m). This

value appears to agree with the single load cases (a) and (b) then the 4-wheel load cases (c) and (d). Still it is quite a surprise that the impact factor for the 4-load case is only $\frac{1}{4}$ to $\frac{1}{3}$ of that for the single load case. However, it is known (4) that initial deflection in the springs has quite an effect on the impact factor. For this reason a fifth loading case (e) is investigated.

The loading case (e) is the same as the loading case (c) except that the springs have an initial displacement of 0.1 ft. (3.05 cm) when the truck is entering the bridge. Modes up to m = 6 and n = 15 have been included. The time increment necessary for convergence is found to be .00035 sec. and the computer running time on Univac 1108 is 35 min. The impact factors in percentages at various points for loading case (e) as compared with those for loading case (c) is given in Table 7.

Table 6. Impact Factor in Percentages
for Loading Case (d) (modes included m = 6,
n = 9)

Point Fig. 9a	a	b_1 b_2	c	d_1 d_2	e_1 e_2	f	g	h
Defl.	5.00	4.74	4.62	4.41	4.51	3.36	4.74	4.51
Long. Stress	4.46	4.63	4.67	4.37	4.51	4.45	4.85	4.38
M_x	6.75	3.07 3.07	1.88	1.13 1.89	3.27 3.84	3.62	*	1.61
M_y	0	* 4.95	0.92	3.24 1.94	4.83 4.36	0	4.59	-1.28

*Static value too small to give meaningful results.

Table 7. Impact Factor in Percentages
for Loading Case (e) as Compared with Those
for Loading Case (c)

Loading & Modes	(e) m = 6, n = 15				(c) m = 6, n = 9			
Point Fig. 9a	a,f	b_1·d_2 b_2·d_1	c	g,h	a,f	b_1·d_2 b_2·d_1	c	g,h
Defl.	177.16	167.35	164.01	167.02	4.73	4.60	4.57	4.60
Long. Stress	152.35	117.13	121.50	141.86	4.43	4.36	4.43	4.31
M_x	133.84	61.03 103.54	71.52	125.93	4.20	3.63 3.52	1.83	1.77
M_y	0	159.02 83.05	37.26	*	0	22.18 7.66	2.51	*

*Static value too small to give meaningful results.

It can be seen from Table 7 that the impact factor is profoundly affected by the initial displacement in the springs. It may be as high as 177% for deflection, 152% for longitudinal stress and 159% for transverse moments. The corresponding values for springs without initial displacement (loading case (c)) are 4.73%, 4.43% and 22.18%, respectively.

An examination of the tables shows that the impact factors for deflections, longitudinal stresses and moments are generally not the same and different for different points. However, with few exceptions (such as M_y at b for loading (c) and M_x at a for loading (d)), it appears that the use of the maximum impact factor for deflection as the impact factor longitudinal stresses and plate moments will give results on the safe side.

A check of the impact percentage obtained for the spring initial displacement case with that obtained from curves given by BIGGS, et al. [4] may be of interest. In the present case, the total moving mass $\hat{M}_V = 4\hat{M}_p = 4 \times 16/32.2 = 1.98$ k-sec²/ft. (29000 kg) and total mass of the bridge = $\hat{M}_B = 23.0 \times .005 \times 100 = 11.5$ k-sec²/ft. (168000 kg). Then $2\hat{M}_V/\hat{M}_B = 0.344$ and frequency of the load = $\omega_p = \sqrt{4\hat{K}_p/4\hat{M}_p} =$

$\sqrt{\dfrac{4 \times 104}{1.98}} = 14.5$ in which $\hat{K}_p$ is the spring constant of each wheel load. The frequency of the bridge for m = 1 and n = 1 is $\omega = 20.2$; see Table 2. Then $\omega/\omega_p = 1.38$ and $\beta = \zeta^p\omega_p^2/g = 0.1 \times 14.5^2/32.2 = 0.65$ in which ζ^p is the initial displacement in the springs. From the curves given in Figure 15 of reference [4], [Note $\hat{M}_V$, $\hat{M}_B$, ζ^p, ω, ω_p correspond respectfully to M_V, $2M_B$, z_m, p_B, p_v in reference [4]], one obtains the ratio of dynamic to static deflection $\Delta_{yd}/\Delta_{ys} = (y_m/y_{st})_1 \times (CF)_\beta \times (CF)_M =$

$1.65 \times 1.37 \times 0.98 = 2.23$. This corresponds to an impact factor of 123% as compared with 177% obtained herein.

The method developed by BIGGS, et al. [4] is also used to check the results for spring borne loads without initial displacement. For loading case (c) with $\beta = 0$, $(CF)_\beta = 0.65$ (extrapolated from the curve) one obtains $\Delta_{yd}/\Delta_{ys} = 1.65 \times 0.65 \times 0.98 = 1.05$. The impact factor of 5% agrees very well with the value of 4.73% obtained herein. In the case of a single wheel load $2\hat{M}_v/\hat{M}_B = 0.344/4 = 0.086$, $(CF)_M = 1.07$, $\Delta_{yd}/\Delta_{ys} = 1.65 \times 0.65 \times 1.07 = 1.15$. The impact factor of 15% agrees fairly well with the value of 19% obtained for loading cases (a) and (b).

Conclusions for Practicing Engineers

Based on the results of this study, the following conclusions may be reached.

1. With limited but sufficient number of modes, the proposed method gives correct results for defections, longitudinal stresses and plate moments at all points except for plate moments at points directly under the concentrated loads. Impact factors and amplification factors obtained from dynamic analysis of the example bridge are sufficiently accurate for the number of modes taken into consideration.

2. With moderate number of plate elements and modes, the larger the length to width ratio of a plate, the poorer will be the values of the plate moments at points directly under the concentrated loads. However, as pointed out in the previous paper [7] the higher the number of modes included, the smaller the time increment (which is proportional to the period of the highest mode) required in a dynamic analysis. Some special method must be developed for determining plate moments at point of application of a concentrated load.

3. As pointed out in one of the examples, inclusion of higher modes may even cause a loss of accuracy due to inaccuracies in the eigenvectors of the higher modes. As pointed out in the previous paper [7], the computer program is based on a method given in reference [17]. It is beyond the scope of this study to make an exhausive evaluation of all available methods. More powerful methods for determining accurate eigenvectors are urgently needed.

4. The impact factors for deflections, longitudinal stresses and plate moments are generally not the same and different for different points. However, with few exceptions, it appears that the use of maximum impact factor for deflection as the impact factor for longitudinal stresses and plate moments will give results on the safe side.

5. The impact factor for a bridge subjected to 4-wheel load may be less than that for the same bridge subjected to a single wheel load.

6. Initial deflection in the spring of the wheel load has profound effect on the impact factor.

7. For the example considered, an estimate of the maximum impact factor for deflection for wheel loads with or without initial displacement in the spring may be made by the method given by BIGGS, et al. [4].

8. As pointed out in the previous paper [7], the study made herein provides better knowledge of the dynamic effects of moving loads on box girder bridges. The information presented herein should be of value to the practicing engineers for providing safety and economy in their design of such bridges.

References

1. American Association for State Highway Officials: Standard Specification for Highway Bridges, Washington, D.C., 1973.
2. American Institute of Steel Construction: Design Manual for Orthotropic Steel Plate Deck Bridges. AISC, New York, N.Y., 1963.
3. ARCHER, J.S.: Consistent Mass Matrix for Distributed Mass Systems, Journal of the Structural Division, ASCE, Vol. 89, No. ST4, Proc. Paper 3591, Aug., 1963, pp. 161-178.
4. BIGGS, J.M., SUER, H.S., and LOUW, J.M.: Vibration of Simple Span Highway Bridges. ASCE Transactions, 1959, Paper No. 2979, pp. 291-318.
5. BOEHNING, R.H.: Single and Tandem Axle Dynamic Effects on a Highway Bridge Model. Civil Engineering Studies, Structural Research Series No. 57, University of Illinois, Urbana, Ill., 1953.
6. CHU, K.H., and DUDNIK, E.: Concrete Box Girder Bridges Analyzed as Folded Plates, First International Symposium Concrete Bridge Design, American Concrete Institute, Publication SP-23, 1969, pp. 221-246.
7. CHU, K.H., and JONES, M.: Theory of Dynamic Analysis of Box Girder Bridges. Memoires of Int. Assoc. of Bridge & Struc. Eng., Vol. 36 II, 1976, p. 121.
8. FENVES, S.J., VELETSOS, A.S., and SIESS, C.P.: Dynamic Studies of the AASHO Road Test Bridges, The AASHO Road Test, Highway Research Board Special Report 73, pp. 83-96.
9. EICHMANN, E.S.: Influence of Vehicle Suspensions on Highway Bridge Impact. Civil Engineering Studies, Structural Research Series No. 70, University of Illinois, Urbana, Ill., 1954.
10. GOLDBERG, J.E., and LEVE, H.L.: Theory of Prismatic Folded Plate Structures. Inter. Assoc. of Bridge and Structural Engineering Publication, Vol. 17, 1957, pp. 59-86.
11. IYENGAR, K.T.S.R., and JAGADISH, K.S.: The Responses of Beam and Slab Bridges to Moving Forces. Inter. Assoc. of Bridge and Structural Engineering Publication, Vol. 28, 1968, p. 69.
12. KENT, M.F.: AASHO Road Test Vehicle Operating Cost Related to Gross Weight. Appendix B, Tire Data, The AASHO Road Test, Highway Research Board Special Report, p. 163.
13. SCRODELIS, A.C., and DEFRIES-SKENE, A.: Direct Stiffness Solution for Folded Plates. Journal of the Structural Division, ASCE, Vol. 90, No. ST4, Proc. Paper 3994, Aug., 1964, pp. 15-47.
14. VELETSOS, A.S., and HUANG, T.: Analysis of Dynamic Response of Highway Bridges. Journal of the Engineering Mechanics Division, ASCE, Vol. 96, No. EM5, Proc. Paper 7591, Oct., 1970, pp. 593-620.
15. TIMOSHENKO, S.P., and WORNOWSKY-KRIEGER, S.: Theory of Plates and Shells, McGraw-Hill Book Company, Inc., New York, N.Y., 1959.
16. TIMOSHENKO, S.P., and YOUNG, D.H.: Vibration Problems in Engineering, D. Van Nostrand Co., Inc., Princeton, N.J., 1955.
17. WILKINSON, J.H.: The Calculation of the Latent Roots and Vectors of Matrices on the Pilot Model of the A.S.E., Proceedings of the Cambridge Philosophical Society, Vol. 50, 1954, pp. 535-566.

Summary

The main purpose of this paper is to present numerical results obtained from a computer program based on a theoretical formulation for the analysis of dynamic responses due to moving loads in all plate elements in simply supported box girder bridges presented in a previous paper. Verification of the computer program was made not only to check out the program but to find out the minimum number of plate strips, the minimum number of modes and the largest time increment to be taken for obtaining reasonable accurate results. Dynamic analysis were performed for an example bridge with five loading cases.

Résumé

Le but principal de l'article est de présenter les résultats numériques obtenus à l'aide d'un programme d'ordinateur basé sur une théorie pour l'analyse des effets dynamiques des charges mobiles dans tous les éléments de plaques de ponts à poutres en caisson tel qu'il est présenté dans l'article antérieur. La vérification du programme d'ordinateur a été opérée à titre de contrôle et pour déterminer le nombre minimum des lames, le nombre minimum des modes et l'augmentation maximum du temps afin d'arriver à des résultats d'une précision suffisante. L'analyse dynamique a été faite pour un pont théorique et pour cinq cas de charges.

Zusammenfassung

Die Nachprüfung des Computerprogrammes erfolgte nicht nur aus Kontroll-gründen, sondern auch um die Mindestzahl von Plattenelementen und Formtypen sowie den grössten Zeitintervall zur Erzielung noch genügend genauer Resultate zu ermitteln. Als Beispiel wird die dynamische Berechnung an einer Brücke für fünf Belastungsfälle durchgeführt. Der Hauptzweck dieses Beitrages besteht darin, rechnerische Resultate eines Computerprogrammes vorzulegen. Dieses Programm stützt sich auf die im vorhergehenden Beitrag behandelte Theorie für die Berechnung von Kastenträgerbrücken unter dynamischen Lasten.

Leere Seite

Blank page

Page vide